March 15, 2002

Thermoelectric properties of the n-type filled skutterudite Ba0.3Co4Sb12 doped with Ni

Jeffrey S. Dyck, *John Carroll University*
Wei Chen, *University of Michigan - Ann Arbor*
Ctirad Uher, *University of Michigan - Ann Arbor*
Lidong Chen
Xinfeng Tang, et al.

Thermoelectric properties of the *n*-type filled skutterudite $Ba_{0.3}Co_4Sb_{12}$ doped with Ni

Jeffrey S. Dyck,[a)] Wei Chen, and Ctirad Uher
Department of Physics, University of Michigan, Ann Arbor, Michigan 48109

Lidong Chen
The State Laboratory of High Performance Ceramics and Superfine Structure, Shanghai Institute of Ceramics, Chinese Academy of Sciences, Shanghai 200050, China

Xinfeng Tang
The State Laboratory of Advanced Technology for Materials Synthesis and Processing, Wuhan University of Technology, Wuhan 430070, China

Toshio Hirai
Institute for Materials Research, Tohoku University, Sendai 980-8577, Japan

Synthesis and electrical and thermal transport properties are reported for several filled skutterudite compounds doped with Ni: $Ba_{0.3}Ni_xCo_{4-x}Sb_{12}$ with $0<x<0.2$. Divalent Ba readily fills the cages of the skutterudite structure and is effective in reducing the thermal conductivity of the structure. The presence of a small amount of Ni increases the electron concentration, further reduces the thermal conductivity, and enhances the thermoelectric power factor. Hall mobility studies indicate that the addition of Ni to the system has the effect of increasing the relative strength of ionized impurity scattering as compared to acoustic phonon scattering. These results suggest that doping with Ni is an attractive avenue to optimization of filled skutterudites. The dimensionless thermoelectric figure of merit *ZT* was observed to increase from a value of 0.8 at 800 K for $Ba_{0.3}Co_4Sb_{12}$ to a value of 1.2 for the sample with $x=0.05$. These materials show considerable potential as *n*-type legs in thermoelectric power generation at elevated temperatures. © *2002 American Institute of Physics.* [DOI: 10.1063/1.1450036]

I. INTRODUCTION

The filled skutterudites based on $CoSb_3$ have been attracting substantial interest because of their promising thermoelectric performance.[1] The properties of the particular filler atom, such as atomic radius, mass, and valence, have considerable influence on the electrical and thermal transport. For example, an undersized filler atom is thought to ''rattle'' about its equilibrium position inside the cagelike voids of the parent binary compound, thereby reducing the lattice thermal conductivity.[2,3] At the same time, the incorporation of these electropositive elements adds electrons to the structure. Filling the voids with La or Ce, and compensating for the excess charge by doping with Fe on the Co site or Sn on the Sb site results in *p*-type samples.[3–6] A dimensionless figure of merit of $ZT=1-1.4$ was found for temperatures between 700 and 1000 K for samples of this type.[6–9] It should be noted, however, that only about 10% of the voids can be filled with Ce (Ref. 4) and up to 23% in the case of La (Ref. 5) without charge compensation, so the ability to obtain *n*-type filled skutterudites has been hampered. Recently, Yb-filled[10] and Tl-filled[11] *n*-type skutterudites with high thermoelectric performance were reported.

In our recent work, we synthesized a series of samples with composition $Ba_yCo_4Sb_{12}$.[12,13] We showed that up to

44% of the voids can be filled with Ba without any charge compensation, and the lattice thermal conductivity was dramatically reduced compared to the unfilled host. The divalent nature of the Ba atoms may be at least partly responsible for the anomalously high filling fraction, donating fewer electrons to the system than trivalent La or Ce. The situation is likely more complicated than simple electron counting for it was found that only 22% of monovalent Tl could be incorporated[11] into the voids of Co_4Sb_{12}, and the question of why the Ba filling fraction is so high is still being pursued. All $Ba_yCo_4Sb_{12}$ samples have respectable thermoelectric properties and the compound $Ba_{0.24}Co_4Sb_{12}$ shows increasing *ZT* with increasing temperature that reaches a value of 1.1 at 850 K. This is one of the highest experimentally determined thermoelectric figures of merit reported for *n*-type skutterudites [compared to extrapolated values of 0.8 at 800 K for $Tl_{0.22}Co_4Sb_{12}$ (Ref. 11) and ~1 at 600 K for $Yb_{0.19}Co_4Sb_{12}$ (Ref. 10)].

One step to realization of higher *ZT* values in these materials is to further tune the electrical properties via doping on the framework structure. Dilley *et al.*[14] recently employed this technique in their study of the thermoelectric properties of $Yb_yCo_4Sn_xSb_{12-x}$. It was found that the compensation of charge in *n*-type samples by substitution of Sn for Sb resulted in lower values of *ZT*, a finding that is similar to studies on other systems. On the other hand, several researchers have noted relatively high thermoelectric performance for unfilled, heavily *n*-type ($10^{20}–10^{21}$ cm^{-3} range)

[a)]Author to whom correspondence should be addressed; electronic mail: jdyck@umich.edu

Co_4Sb_{12} achieved by substituting Ni, Pt, or Pd for Co[15–17] or Te for Sb.[15,18] These factors suggest that *n*-type doping rather than charge compensation of an *n*-type filled skutterudite may be beneficial. Small amounts of Ni in Co_4Sb_{12} have an attractive effect of lowering the total thermal conductivity and increasing the electrical conductivity.[19,20] In early investigations by Dudkin and Abrikosov,[19] it was concluded that the presence of up to 1 at. % Ni "corrects" structural distortions in the lattice, resulting in increased microhardness and carrier mobility.

The aim of the present work is to ascertain the effect of Ni on the properties of $Ba_yCo_4Sb_{12}$. The wide filling space of Ba ($y=0-0.44$) makes it an ideal candidate for this study since it is not expected that the addition of electrons to a partially filled compound will exclude the Ba atoms. The results are analyzed within a model of mixed acoustic lattice and ionized impurity carrier scattering.

II. EXPERIMENT

Polycrystalline samples having compositions $Ba_yNi_xCo_{4-x}Sb_{12}$ with $y\approx 0.3$ and $0<x<0.2$ were prepared as follows. Highly pure metals of Ba (99.9%, plate), Sb (99.9999%, powder), Ni (99.9%, powder), and Co (99.99%, powder) were used as the starting materials. Because the reaction between Ba and Sb or Co is highly exothermic, it is difficult to directly melt or react a mixture of the constituent elements. In the present study, a two-step solid reaction was used. A binary compound of $BaSb_3$ and a ternary compound of $Ni_xCo_{1-x}Sb_2$ were first synthesized by reacting the constituent elements in a flowing Ar atmosphere. Reaction temperature and reaction time were 903 K for 72 h and 973 K for 168 h for the synthesis of $BaSb_3$ and $Ni_xCo_{1-x}Sb_2$, respectively. For the synthesis of a $BaSb_3$ compound, it is important that the samples be heated slowly (<1 K/min) from room temperature to 793 K and be kept at that point for 12 h before being heated to the reaction temperature (903 K). The resulting compounds, $BaSb_3$ and $Ni_xCo_{1-x}Sb_2$, were then crushed and mixed with Sb in various $Ba:(Ni+Co):Sb$ $=y:4:12$ molar ratios and pressed into pellets. The pellets were heated and reacted three times at 973 K under an Ar atmosphere for 72 h. The reacted materials were milled into fine powder and washed with $HCl+HNO_3$ to remove a slight amount of impurity phases (Sb and $Ni_xCo_{1-x}Sb_2$). To form a fully dense polycrystalline solid, the obtained powder was sintered by the plasma activated sintering method. Sintering was performed at a temperature of 873 K for 15 min.

The skutterudite phase of the samples was verified by powder x-ray diffractometry (Rigaku: RAD-C, Cu $K\alpha$). The crystalline structure was refined by using a Rietveld crystallographic analysis program. Chemical compositions were determined by electron probe microanalysis and inductively coupled plasma emission spectroscopy.

The measurement of thermal conductivity κ, thermopower S, and electrical resistivity ρ at low temperatures (2–300 K) was carried out in a cryostat equipped with two radiation shields. A steady-state longitudinal method was employed and typical sample dimensions were $3\times 3\times 10$ mm^3. Thermal gradients were measured with the aid of

fine copper–constantan thermocouples, with a miniature strain gauge serving as a heater. The copper legs of the thermocouples were used as voltage probes for resistivity and thermopower measurements, and the Seebeck coefficients were corrected for the contribution from the Cu wires.[21,22] Radiation loss is an unfortunate and unavoidable error in all thermal conductivity measurements made using a longitudinal steady-state technique manifested by deviations from the true value that increase with temperature above about 200 K. In order to determine the radiation loss experimentally, we made a subsequent measurement with the sample detached from the heat sink (sample hangs by its thin connecting wires) and determined the amount of heat needed to supply to the heater that raises the temperature of the entire sample to the same average temperature as during the actual measurement of the thermal conductivity. The values of the thermal conductivity were then corrected for this radiation loss. The magnitude of the correction was typically around 10% of the total thermal conductivity for these samples at 300 K. Hall effect and additional resistivity measurements were performed in a Quantum Design superconducting quantum interference device magnetometer system with 5.5 T magnet using a Linear Research ac bridge with 16 Hz excitation on small specimens cut from the large ones used for thermal transport measurements. Data were taken in both positive and negative magnetic fields to eliminate effects due to any probe misalignment. The absolute uncertainty in all the measured transport parameters is estimated to be less than 5%, limited primarily by the measurement of probe separations.

For measurements over the temperature range of 300–900 K, the thermoelectromotive force ΔE was measured at five different temperature gradients ($0\leqslant \Delta T\leqslant 10$ K), and the Seebeck coefficient was obtained from the slope of the ΔE versus ΔT plot. High temperature thermal conductivity was measured by a laser flash method (Shinkuriko: TC-7000) in vacuum.

III. RESULTS AND DISCUSSION

Temperature dependence of the electrical resistivity for the $Ba_{0.3}Ni_xCo_{4-x}Sb_{12}$ samples is shown in Fig. 1. The electrical behavior of all samples shows metallic temperature dependence, which is expected from a heavily doped (degenerate) semiconductor. At room temperature, the resistivity first drops as the concentration of Ni increases up to $x\sim 0.1$, and then begins to increase. From the room temperature value of the Hall coefficient, we calculated the carrier concentration using the equation $R_H=A/ne$, where A is the Hall factor which depends in general on the scattering mechanism and degree of degeneracy. A does not differ from 1 by more than 10% for degenerate systems[23] (a condition we establish below), so we take it to be 1. Figure 2 shows that the carrier concentration increases as the Ni content increases.

The thermopower S and thermal conductivity κ are displayed as a function of temperature in Figs. 3 and 4, respectively. All samples have negative S with a nearly linear increase in magnitude with temperature, aspects which are consistent with degenerate electron transport. The most surprising thing about this data is that, although the carrier con-
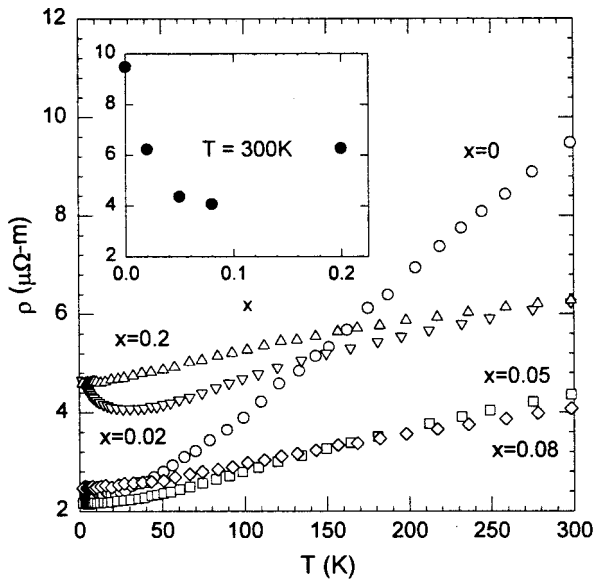
FIG. 1. Temperature dependence of the electrical resistivity from 2 to 300 K for $Ba_{0.3}Ni_xCo_{4-x}Sb_{12}$. The inset shows the resistivity as a function of Ni concentration at 300 K.

FIG. 3. Seebeck coefficient vs temperature for $Ba_{0.3}Ni_xCo_{4-x}Sb_{12}$.

centration increases by a factor of 3 over the range of x studied, the room temperature S values do not change by more than 10%. In fact, $|S|$ increases marginally as the Ni concentration increases from $x=0.02$ to $x=0.2$. The room temperature thermal conductivity values for the $Ba_{0.3}Ni_xCo_{4-x}Sb_{12}$ samples range from 3.8 to 4.5 W/m K, and are not strongly temperature dependent down to 50 K. Also shown in Fig. 4 are data for two other Ba-filled Co_4Sb_{12} samples without Ni and with lower Ba filling fractions. These data illustrate the strong effect the Ba occupancy has on κ both at room temperature and at the peak near 60 K. The subsequent effect of Ni for fixed Ba content is not as dramatic, although κ is minimized for $x=0.05$.

Temperature dependence of the Hall mobility $\mu_H = R_H/\rho$ is shown in Fig. 5. Room temperature values are approximately 10 cm²/V s, which are somewhat higher than that for Ce or La-filled skutterudites with comparable carrier concentrations.[6,7,24] From the temperature dependence of the Hall mobility we can gain some insight into the carrier scat-
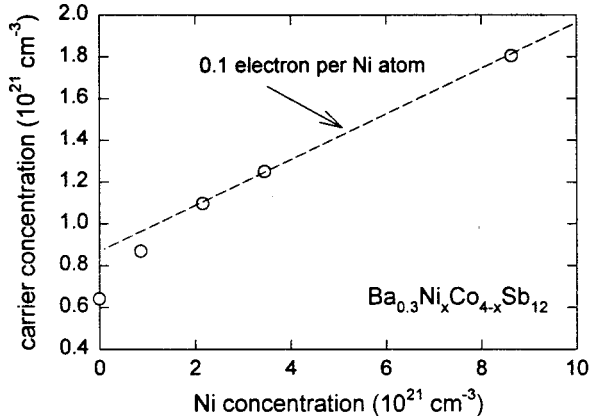
tering mechanisms. As a frame of reference, we analyze the behavior of μ_H for a series of samples $Ba_yCo_4Sb_{12}$ without Ni [see Fig. 5(a)]. The Ni-free samples cover a comparable carrier concentration range to those of the Ni-doped samples. For all of the Ba-filled skutterudites without Ni, μ_H follows a $T^{-3/2}$ dependence near room temperature, and saturates to a constant value below about 20 K. This behavior is suggestive of a combination of scattering by acoustic phonons at high temperature, and neutral impurities below 20 K. The case is clearly different for the samples containing Ni [see Fig. 5(a)]. As the Ni concentration increases, the slopes of the μ_H versus T curves near room temperature become distinctly less negative, indicating the presence of more than one dominant scattering mechanism within a picture of a single, rigid band. Because Ni acts as an electron donor in this system, there will be additional scattering due to ionized impurities. Likewise, barium atoms donate electrons to the

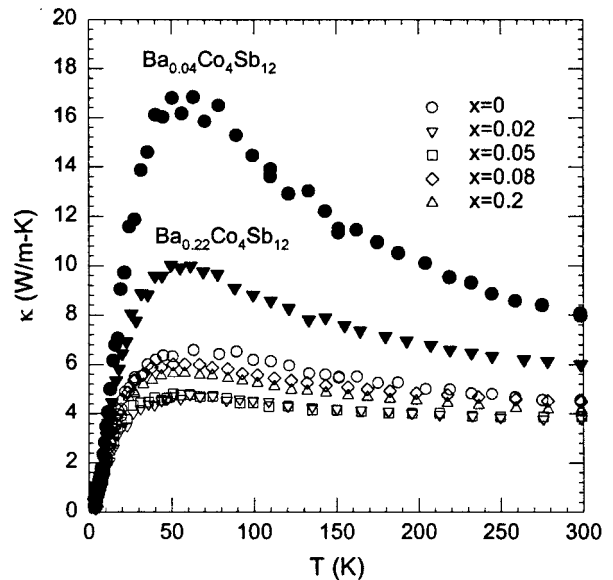FIG. 2. Hall electron concentration vs Ni content at room temperature for $Ba_{0.3}Ni_xCo_{4-x}Sb_{12}$.

FIG. 4. Total thermal conductivity vs temperature for $Ba_{0.3}Ni_xCo_{4-x}Sb_{12}$ (open symbols). Also shown are two samples without Ni but lower concentrations of Ba (filled symbols).
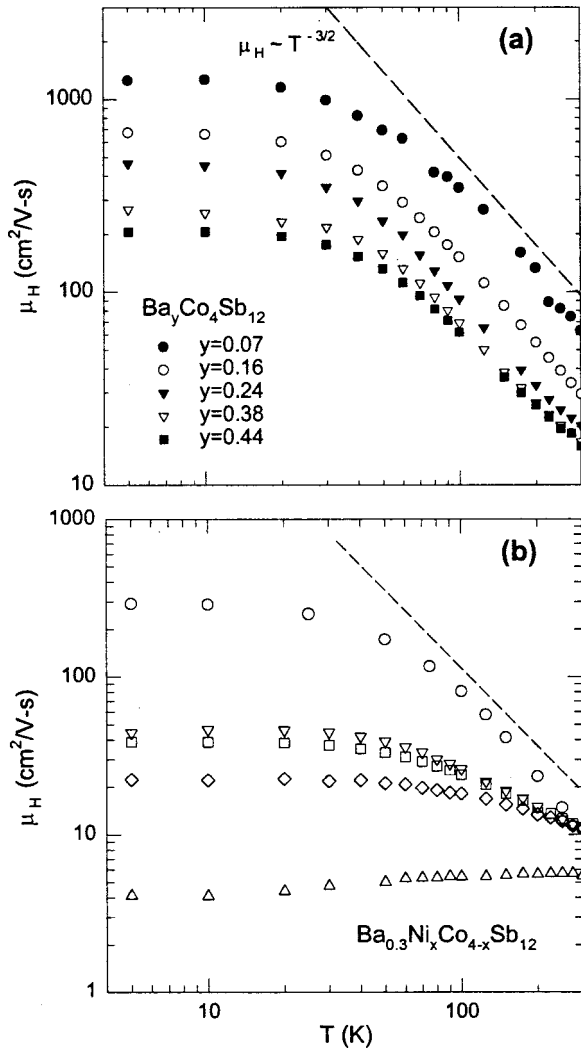
FIG. 5. Temperature dependence of the Hall mobility (R_H/ρ) for (a) $Ba_yCo_4Sb_{12}$ and (b) $Ba_{0.3}Ni_xCo_{4-x}Sb_{12}$. Symbol definitions for (b) are the same as in Fig. 4. The dashed lines show a $T^{-3/2}$ dependence expected from purely acoustic lattice scattering.

system, and therefore have a net positive charge. However, there is a clear distinction in this case since these atoms are understood to reside inside the oversized cages. Provided the charge transport takes place primarily on the Co_4Sb_{12} framework, it is feasible that the carriers are not strongly affected by the charged filler atoms.

To describe the influence of Ni on the transport properties, we consider a model of mixed carrier scattering. In this case, the mobility depends on two relaxation times: one corresponds to scattering of electrons by acoustic vibrations $\tau_L = \tau_{0L}\varepsilon^{-1/2}$, and the other one is due to scattering on ionized impurity atoms $\tau_i = \tau_{0i}\varepsilon^{3/2}$. Here, ε is the reduced carrier energy. It is easily shown that a combined relaxation time τ can be expressed as

$$\tau = \frac{\tau_{0L}\varepsilon^{3/2}}{\varepsilon^2 + a^2}, \tag{1}$$

where

$$a = \sqrt{\frac{\tau_{0L}}{\tau_{0i}}}. \tag{2}$$

The relevant transport equations in the relaxation time approximation for mixed lattice and ionized impurity scattering are[23]

$$\sigma = \frac{1}{\rho} = \frac{8\pi e^2}{3m^*h^3}(2m^*k_BT)^{3/2}\tau_{0L}\Phi_3(\eta,a), \tag{3}$$

$$R_H = \frac{3h^3}{8\pi e(2m^*k_BT)^{3/2}}\frac{\Phi_{9/2}(\eta,a)}{[\Phi_3(\eta,a)]^2}, \tag{4}$$

$$S = -\frac{k_B}{e}\left[\frac{\Phi_4(\eta,a)}{\Phi_3(\eta,a)} - \eta\right], \tag{5}$$

where m^* is the effective mass, k_B is Boltzmann's constant, h is Planck's constant, e is the electronic charge, η is the reduced Fermi energy, and

$$\Phi_{m,\text{integer}}(\eta,a) = \int_0^\infty \frac{\varepsilon^m\exp(\varepsilon-\eta)}{(\varepsilon^2+a^2)[1+\exp(\varepsilon-\eta)]^2}d\varepsilon, \tag{6}$$

$$\Phi_{9/2}(\eta,a) = \int_0^\infty \frac{\varepsilon^{9/2}\exp(\varepsilon-\eta)}{(\varepsilon^2+a^2)^2[1+\exp(\varepsilon-\eta)]^2}d\varepsilon. \tag{7}$$

Furthermore, the carrier concentration n can be expressed as

$$n = 4\pi\left(\frac{2m^*k_BT}{h^2}\right)^{3/2}F_{1/2}(\eta), \tag{8}$$

where $F_{1/2}(\eta)$ is the Fermi function. Equations (4) and (5), in principle, represent the tools necessary to determine the scattering parameter a and reduced Fermi energy η. However, one must know m^* to simultaneously solve the equations given the experimental transport parameters. Again, to understand the underlying behavior, we first determine m^* for the samples without Ni.

Given that the Hall mobility data for $Ba_yCo_4Sb_{12}$ seem to unambiguously indicate acoustic lattice scattering is dominant at room temperature, we calculated the effective mass as a function of carrier concentration for this system in the limit $a\rightarrow 0$. From Eq. (5) we find η and, together with the Hall carrier concentration, solve Eq. (8) for m^*. These results are shown in Fig. 6 (open circles) and indicate that m^* increases with carrier concentration. Also shown are the effective masses calculated for the $Ba_{0.3}Ni_xCo_{4-x}Sb_{12}$ samples calculated under the same assumption of the dominance of acoustic phonon scattering, i.e., as $a\rightarrow 0$. Acoustic lattice scattering is commonly cited as the dominant scattering mechanism near room temperature in filled and unfilled skutterudites.[3,7,11,16] If this assumption were made here, the calculated effective mass depicted in Fig. 6 increases to $m^* = 7m_0$ upon addition of Ni, suggesting a strong influence on the band structure. This is unlikely for such small concentrations of impurity. Therefore, in order to proceed, we make the assumption that the dominant effect of Ni on this system is to add electrons and increase ionized impurity scattering within a rigid band approximation.

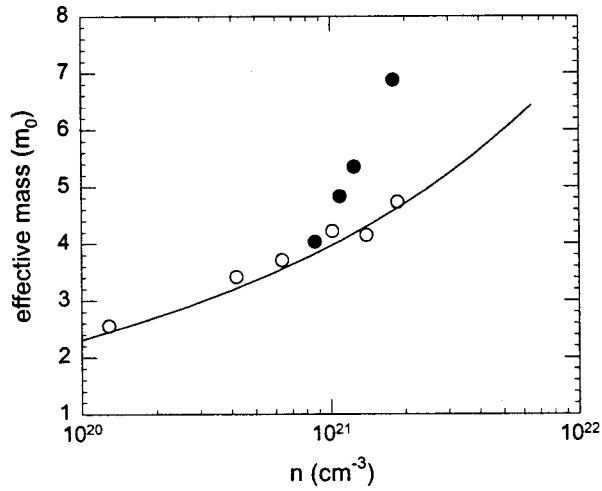As others have noted,[15,16] the carrier concentration is well described in terms of a two-band Kane model:

FIG. 6. Effective mass as a function of carrier concentration for $Ba_{0.3}Ni_xCo_{4-x}Sb_{12}$ (filled symbols) and $Ba_yCo_4Sb_{12}$ (open symbols) calculated assuming acoustic lattice scattering and a single parabolic band. The solid line is a fit of the $Ba_yCo_4Sb_{12}$ data to the Kane model given by Eq. (9) with $m_b^* = 2m_0$ and $E_g = 0.175$.
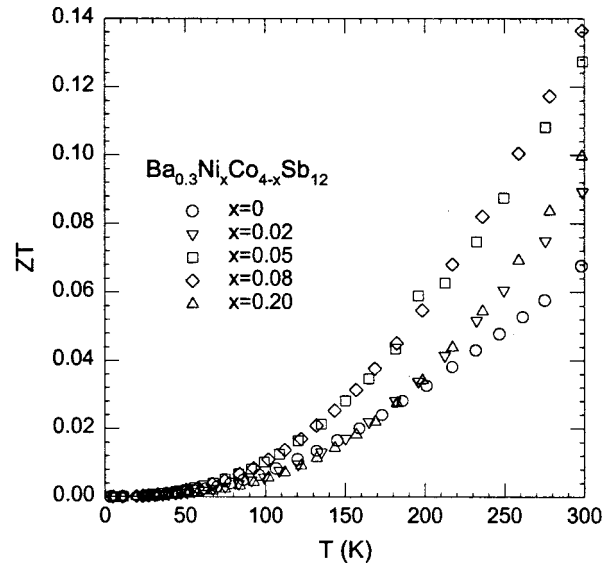

FIG. 7. Dimensionless thermoelectric figure of merit ZT as a function of temperature from 5 to 300 K for Ni-doped Ba-filled skutterudites.

$$m^* = m_b^* \left(1 + \frac{2\eta}{\Delta} \right), \qquad (9)$$

where m_b^* is the effective mass at the bottom of the band and $\Delta = E_g/k_BT$ is the reduced band gap energy. The observed changes in effective mass are compared to the Kane model by using Eq. (9) with $E_g = 0.175$ eV and $m_b^* = 2m_0$ and the agreement is quite good. These results for effective mass concur with prior experiments.[11,16,24] Additionally, band structure calculations have shown that the bands close to the Fermi level are well described by the Kane model and have predicted a band gap of 0.22 eV.[25] Having established the relationship of effective mass to reduced Fermi energy, we can determine room temperature values of a for the Ni doped samples. The values of a and η as calculated from Eqs. (4), (5), and (9) are given in Table I. From this analysis, the parameter a increases from an initial value of 0.5 for samples with no Ni content to a value of 3.3 for samples with the highest Ni content, indicating a smooth crossover from transport dominated by acoustic lattice scattering to that dominated by ionized impurity scattering. This increase in a corresponds to a ~40-fold decrease of τ_{0i} relative to that of τ_{0L}.

Figure 7 depicts the beneficial effect of Ni on the thermoelectric figure of merit ZT ($= S^2\sigma T/\kappa$) observed for $Ba_{0.3}Ni_xCo_{4-x}Sb_{12}$. ZT at room temperature increases significantly up to Ni concentrations of $x = 0.05$ and then diminishes. This can be understood qualitatively within the mixed scattering model from the standpoint of the power factor $S^2\sigma$. If one simply plots the square of Eq. (5) multiplied by Eq. (3), it is evident (see Fig. 8) that increasing the relative strength of ionized impurity scattering enhances the power factor provided the Fermi level is not increased too much. This is an important feature, because the ability to tailor carrier scattering in a thermoelectric can be used as a tool to optimize its performance. The calculations in Fig. 8 do not take into account the change in effective mass with doping level (Fermi level), which would bring the relative magnitudes of the three curves closer together.

The lattice thermal conductivity κ_L can be calculated by subtracting the electronic contribution via the Wiedemann–Franz law from the total thermal conductivity. The Lorenz number L in the mixed scattering model is

$$L = \left(\frac{k_B}{e} \right)^2 \frac{\Phi_4(\eta,a)^2 - \Phi_3(\eta,a)\Phi_5(\eta,a)}{\Phi_3(\eta,a)^2}. \qquad (10)$$

TABLE I. Room temperature transport parameters for $Ba_{0.3}Ni_xCo_{4-x}Sb_{12}$.

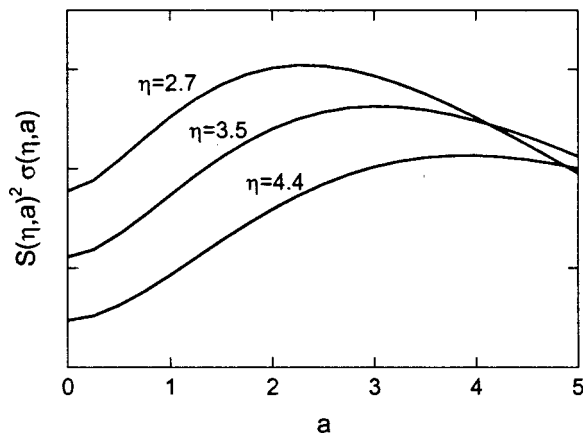|	$Ba_{0.3}Co_4Sb_{12}$	$Ba_{0.3}Ni_{0.02}Co_{3.98}Sb_{12}$	$Ba_{0.3}Ni_{0.05}Co_{3.95}Sb_{12}$	$Ba_{0.3}Ni_{0.08}Co_{3.92}Sb_{12}$	$Ba_{0.3}Ni_{0.2}Co_{3.8}Sb_{12}$
ρ ($\mu\Omega$ m)	8.99	6.67	5.15	4.60	6.24
n (cm^{-3})	6.40×10^{20}	8.68×10^{20}	1.10×10^{21}	1.25×10^{21}	1.82×10^{21}
μ_H (cm^2/V s)	10.84	10.82	11.08	10.84	5.50
S (μV/K)	-97.96	-88.23	-90.31	-91.37	-93.13
κ_L (W/m K)	3.90	2.92	2.75	3.22	3.16
m^* (m_0)	3.50	3.77	4.02	4.17	4.58
η	2.68	3.12	3.48	3.70	4.40
a	4.48	0.58	1.33	1.79	3.33
L (V^2/K^2)	1.90×10^{-8}	1.95×10^{-8}	1.95×10^{-8}	1.96×10^{-8}	2.02×10^{-8}

FIG. 8. Dependence of the power factor (S^2/ρ) on the degree of ionized impurity scattering as expressed by the parameter a for several values of the reduced Fermi level η using Eqs. (3) and (5).

Values of L calculated using Eq. (10) are approximately 20% smaller than the Sommerfeld value of 2.44×10^{-8} V^2/K^2, and reflect the partial inelasticity of the carrier scattering. Resulting room temperature lattice thermal conductivities as a function of Ni concentration are given in Table I. Addition of Ni to Ba$_{0.3}$Co$_4$Sb$_{12}$ suppresses the lattice thermal conductivity relative to the Ni-free sample, and a minimum value of 2.75 W/m K is obtained for $x=0.05$. We and others have observed a significant reduction of κ_L in

Ni$_x$Co$_{1-x}$Sb$_3$.[11,16,20] In these studies, the dominant phonon scattering mechanism was attributed to electron–phonon interaction.

The room temperature ZT value is obviously too small to be of interest for thermoelectric applications at these temperatures, though the trend with addition of Ni is encouraging. It is therefore imperative to experimentally determine the transport properties at high temperatures. Figure 9 illustrates the transport properties and ZT over the temperature range 300–800 K. The agreement at room temperature between the two sets of data is within 20% with the exception of the ρ value for the $x=0$ sample. This mismatch of the data at room temperature arises from the use of different experimental methods (ac versus dc technique and very different techniques to determine thermal conductivity) for the low temperature and high temperature data sets. However, we observe that the overall trends are preserved, and that this is so up to 800 K.

At elevated temperatures, the electrical resistivity continues to increase with temperature for all samples containing Ni. The resistivity of Ba$_{0.3}$Co$_4$Sb$_{12}$ peaks near 500 K and then begins to decrease. This downturn is likely associated with the onset of intrinsic conduction in this material. As the carrier concentration is increased due to the presence of Ni, the Fermi level is forced deeper into the conduction band, and hence the resistivity for the samples containing Ni does not reach a maximum up to the highest temperatures. At the same time, the increasing carrier concentration systemati-
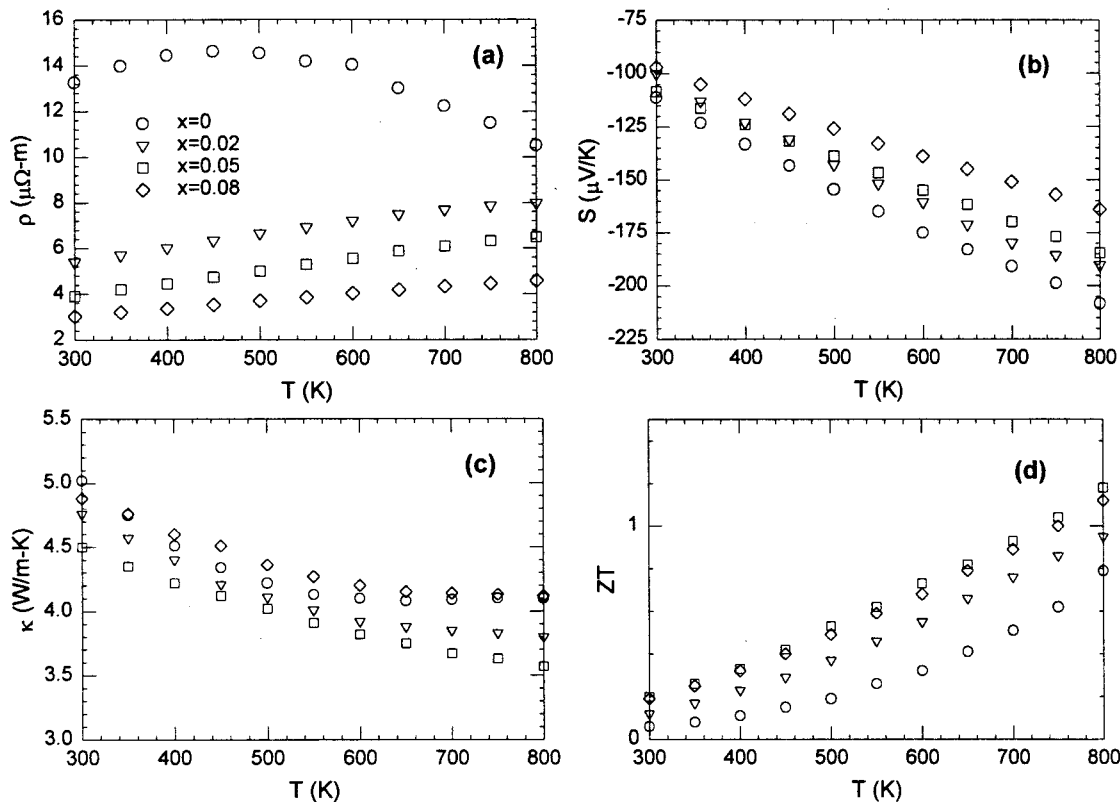

FIG. 9. Temperature dependence of the electrical resistivity (a), Seebeck coefficient (b), total thermal conductivity (c), and dimensionless figure of merit ZT (d) from 300 to 800 K for Ba$_{0.3}$Ni$_x$Co$_{4-x}$Sb$_{12}$ with $0<x<0.08$.
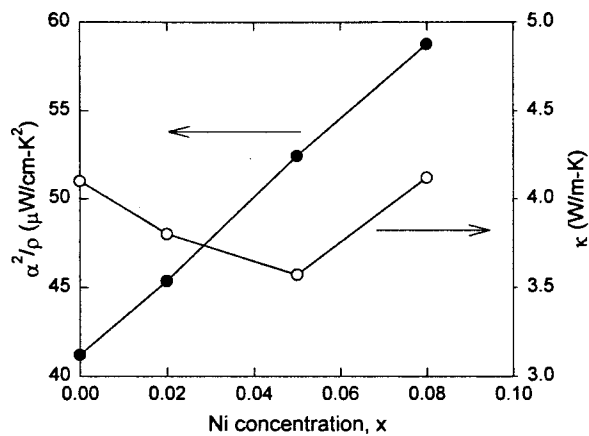
FIG. 10. Power factor and total thermal conductivity at 800 K as a function of Ni content x.

cally lowers the magnitude of the Seebeck coefficient. With increasing temperature, we expect acoustic phonon scattering to begin to dominate [$a(T)$ decreases], therefore the effect of ionized impurity scattering in enhancing the thermopower for Ni-doped samples is not as strong as it is at room temperature. However, the heavy electron masses help to sustain robust values of S. Although Seebeck values are decreasing with increasing x, power factors at 800 K are increasing as can be seen in Fig. 10.

Thermal conductivity values at 800 K for the $Ba_{0.3}Ni_xCo_{4-x}Sb_{12}$ samples are also shown in Fig. 10, and a minimum is found near $x=0.05$. Based on the value of the Lorenz number calculated at 300 K, the electronic thermal conductivity is estimated to be up to 70% of the total thermal conductivity at 800 K for $Ba_{0.3}Ni_{0.05}Co_{3.95}Sb_{12}$. With resistivity values that increase roughly linearly with temperature, we expect the electronic thermal conductivity to be nearly independent of temperature. Then the dominant effect producing the temperature variation in the thermal conductivity is from the contribution of the lattice. Indeed, the decreasing trend with temperature is consistent with Umklapp scattering of phonons. As Ni is added to the structure, the thermal conductivity is further suppressed likely via increased electron–phonon interaction. However, the electronic contribution begins to dominate for the highest Ni content sample, and eventually causes the total thermal conductivity to increase and overall performance to decrease.

Finally, ZT increases monotonically with increasing temperature for all samples with no hint of reaching a maximum even at 800 K. At temperatures much above 1000 K, filled skutterudites based on the Co_4Sb_{12} framework decompose peritectically ($T_p=1146$ K).[26] ZT increases from 0.8 for $Ba_{0.3}Co_4Sb_{12}$ to 1.2 for $Ba_{0.3}Ni_{0.05}Co_{3.95}Sb_{12}$ at 800 K demonstrating the beneficial effect of a small amount of Ni impurity. The nature of the doping effect due to Ni is such that: (1) it acts as an electron donor, thereby increasing electrical conductivity; (2) effective masses increase with Ni concentration; (3) lattice thermal conductivity is diminished, likely due to increased electron–phonon interaction; and (4) the strength of ionized impurity scattering is increased relative to that due to acoustic phonons, especially at lower tempera-

tures. All of these factors help to increase the thermoelectric performance.

IV. SUMMARY AND CONCLUSIONS

Barium-filled skutterudites doped with Ni ($Ba_{0.3}Ni_xCo_{4-x}Sb_{12}$ with $0<x<0.2$) have been synthesized. Electrical transport of all of the samples is consistent with that of a degenerately doped semiconductor. Hall mobility studies indicate that the carrier scattering in samples without Ni, $Ba_yCo_4Sb_{12}(0<y<0.44)$, is dominated by acoustic phonons near room temperature. The addition of Ni results in an increase of the room temperature carrier concentration, giving rise to ionized impurities which influence the mobility and affect the transport properties by changing the relative influence of scattering due to acoustic phonons and ionized impurities. Effective masses also rise due to the doping effect. The dimensionless thermoelectric figure of merit ZT increases from 0.8 for $x=0$ to 1.2 for $x=0.05$ at $T=800$ K. We attribute this enhancement of ZT to both the doping effect of Ni and the accompanying increase of the ionized impurity scattering. These beneficial effects due to the presence of a minute amount of Ni may not be unique to the $Ba_yCo_4Sb_{12}$ system. Therefore these results highlight the need to investigate Ni doping in other Co_4Sb_{12}-based filled skutterudite materials as a possible means to enhance the thermoelectric performance of these materials.

[1] C. Uher, in *Semiconductors and Semimetals*, Vol. 69, Recent Trends in Thermoelectric Materials Research, edited by T. M. Tritt (Academic, San Diego, 2000), pp. 139–253; G. S. Nolas, D. T. Morelli, and T. Tritt, Annu. Rev. Mater. Sci. **29**, 89 (1999).

[2] G. A. Slack and V. G. Tsoukala, J. Appl. Phys. **76**, 1665 (1994).

[3] D. T. Morelli and G. P. Meisner, J. Appl. Phys. **77**, 3777 (1995).

[4] B. Chen, J.-H. Xu, C. Uher, D. T. Morelli, G. P. Meisner, J.-P. Fleurial, T. Caillat, and A. Borshchevsky, Phys. Rev. B **55**, 1476 (1997).

[5] G. S. Nolas, J. L. Cohn, and G. A. Slack, Phys. Rev. B **58**, 164 (1998).

[6] B. C. Sales, D. Mandrus, B. C. Chakoumakos, V. Keppens, and J. R. Thompson, Phys. Rev. B **56**, 15081 (1997).

[7] J.-P. Fleurial, A. Borshchevsky, T. Caillat, D. T. Morelli, and G. P. Meisner, *Proceedings of the Fifteenth International Conference on Thermoelectrics* (IEEE, Pasadena, CA, 1996), p. 91.

[8] B. C. Sales, D. Mandrus, and R. K. Williams, Science **272**, 1325 (1996).

[9] X. Tang, L. Chen, T. Goto, and T. Hirai, J. Mater. Res. **16**, 837 (2001).

[10] G. S. Nolas, M. Kaesar, R. T. Littleton IV, and T. M. Tritt, Appl. Phys. Lett. **77**, 1855 (2000).

[11] B. C. Sales, B. C. Chakoumakos, and D. Mandrus, Phys. Rev. B **61**, 2475 (2000).

[12] L. D. Chen, T. Kawahara, X. F. Tang, T. Goto, T. Hirai, J. S. Dyck, W. Chen, and C. Uher, J. Appl. Phys. **90**, 1864 (2001).

[13] L. Chen, X. Tang, T. Goto, and T. Hirai, J. Mater. Res. **15**, 2276 (2000).

[14] N. R. Dilley, E. D. Bauer, M. B. Maple, and B. C. Sales, J. Appl. Phys. **88**, 1948 (2000).

[15] T. Caillat, A. Borshchevsky, and J.-P. Fleurial, J. Appl. Phys. **80**, 4442 (1996).

[16] H. Anno, K. Matsubara, Y. Notohara, T. Sakakibara, and H. Tashiro, J. Appl. Phys. **86**, 3780 (1999).

[17] K. Matsubara, T. Iyanaga, T. Tsubouchi, K. Kishimoto, and T. Koyanagi, AIP Conf. Proc. **316**, 226 (1995).

[18] Y. Nagamoto, K. Tanaka, and T. Koyanagi, *17th International Conference on Thermoelectrics* (IEEE, New York, 1998), p. 302.

[19] L. D. Dudkin and N. Kh. Abrikosov, Zh. Neorg. Khim. **2**, 212 (1957).

[20] C. Uher, J. S. Dyck, W. Chen, G. P. Meisner, and J. Yang, in *Thermoelectric Materials 2000—The Next Generation Materials for Small-Scale Refrigeration and Power Generation Applications*, edited by T. M. Tritt, G. S. Nolas, G. D. Mahan, D. Mandrus, and M. G. Kanatzidis (Materials

Research Society, Warrendale, PA, 2001), p. Z10.3.1.

[21] R. B. Roberts, Philos. Mag. **36**, 91 (1977).

[22] C. Uher, J. Appl. Phys. **62**, 4636 (1987).

[23] V. I. Fistul, *Heavily Doped Semiconductors* (Plenum, New York, 1969).

[24] D. T. Morelli, G. P. Meisner, B. Chen, S. Hu, and C. Uher, Phys. Rev. B **56**, 7376 (1997).

[25] J. O. Sofo and G. D. Mahan, Phys. Rev. B **58**, 15620 (1998).

[26] P. Feschotte and D. Lorin, J. Less-Common Met. **155**, 255 (1989).